

15. Magnetism

Nov 21, 2019

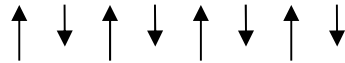
Ferrimagnets

Magnetite Fe_3O_4
(Magneteseisen)



Ferrites $\text{MO}\cdot\text{Fe}_2\text{O}_3$

M = Fe, Zn, Cd, Ni, Cu,
Co, Mg



Two sublattices A and B.

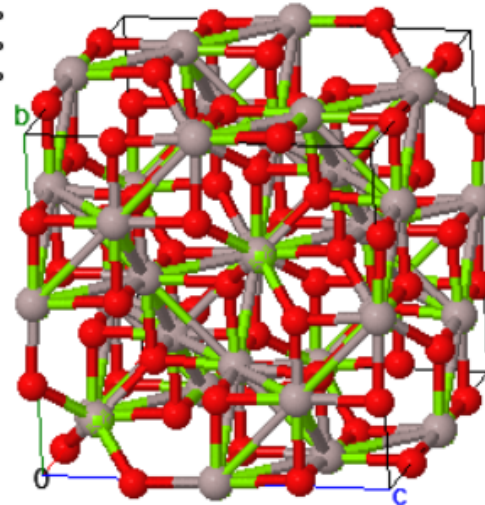
Spinel crystal structure XY_2O_4

8 tetrahedral sites A (surrounded by 4 O) $5\mu_B$ ↑

16 octahedral sites B (surrounded by 6 O) $9\mu_B$ ↓

per unit cell

HM: F d -3 m :2
a=8.084Å
b=8.084Å
c=8.084Å
α=90.000°
β=90.000°
γ=90.000°



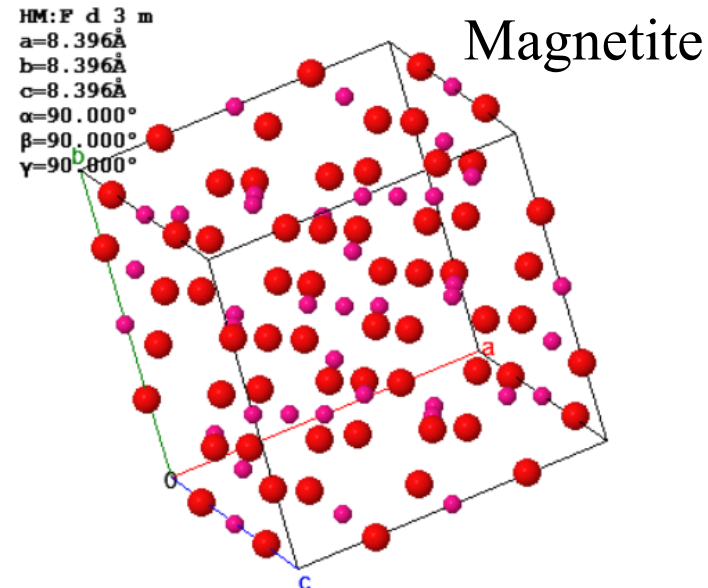
MgAl_2O_4

Ferrimagnets

Magnetite Fe_3O_4

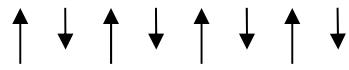
Ferrites $\text{MO}\cdot\text{Fe}_2\text{O}_3$

M = Fe, Zn, Cd, Ni,
Cu, Co, Mg



Exchange integrals J_{AA} , J_{AB} , and J_{BB} are all negative (antiparallel preferred)

$$|J_{AB}| > |J_{AA}|, |J_{BB}|$$



Ferrimagnetism

$$\text{gauss} = 10^{-4} \text{ T}$$

$$\text{oersted} = 10^{-4}/4\pi \times 10^{-7} \text{ A/m}$$

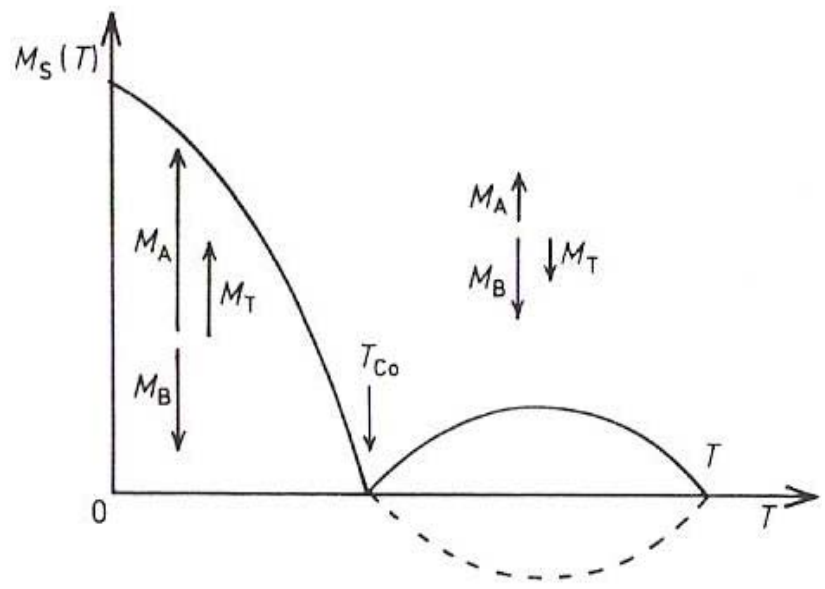


Table 33.3
SELECTED FERRIMAGNETS, WITH CRITICAL TEMPERATURES T_c AND SATURATION MAGNETIZATION M_0

MATERIAL	T_c (K)	M_0 (gauss) ^a
Fe_3O_4 (magnetite)	858	510
CoFe_2O_4	793	475
NiFe_2O_4	858	300
CuFe_2O_4	728	160
MnFe_2O_4	573	560
$\text{Y}_3\text{Fe}_5\text{O}_{12}$ (YIG)	560	195

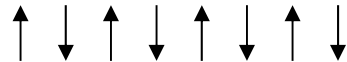
^a At $T = 0(\text{K})$.
 Source: F. Keffer, *Handbuch der Physik*, vol. 18, pt. 2, Springer, New York, 1966.

Kittel

D. Gignoux, magnetic properties of Metallic systems

Antiferromagnetism

Negative exchange energy $J_{AB} < 0$.



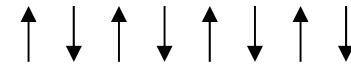
At low temperatures, below the Neel temperature T_N , the spins are aligned antiparallel and the macroscopic magnetization is zero.

Spin ordering can be observed by neutron scattering.

At high temperature antiferromagnets become paramagnetic. The macroscopic magnetization is zero and the spins are disordered in zero field.

$$\chi = \mu_0 \frac{\vec{M}_A + \vec{M}_B}{\vec{B}_a} = \frac{C}{T + \Theta} \quad \leftarrow \text{Curie-Weiss temperature}$$

Antiferromagnetism



Average spontaneous magnetization is zero at all temperatures.

Source: Kittel

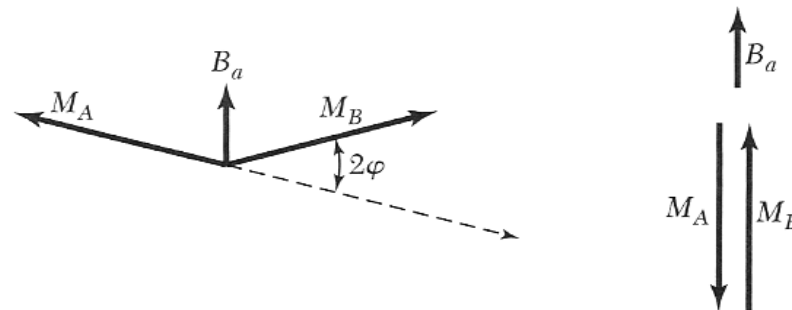
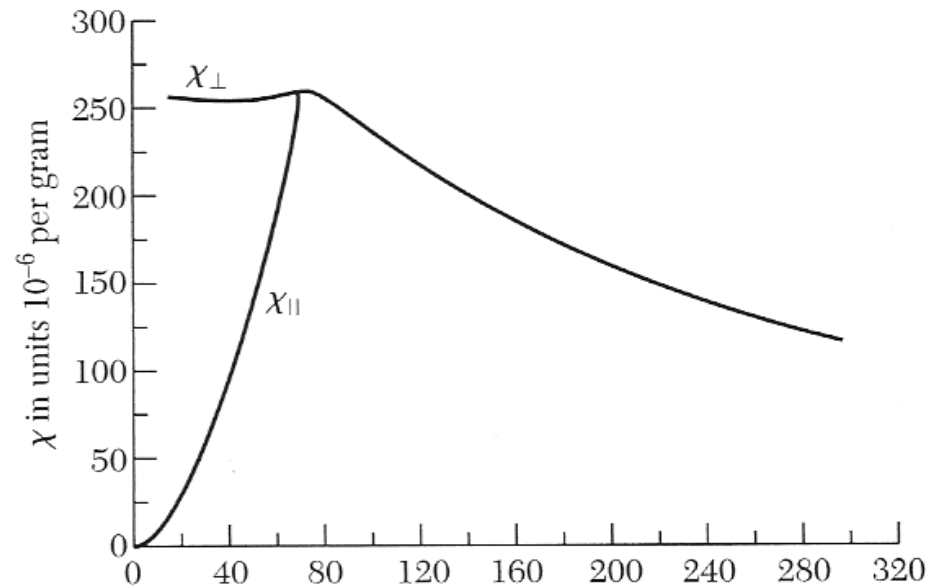
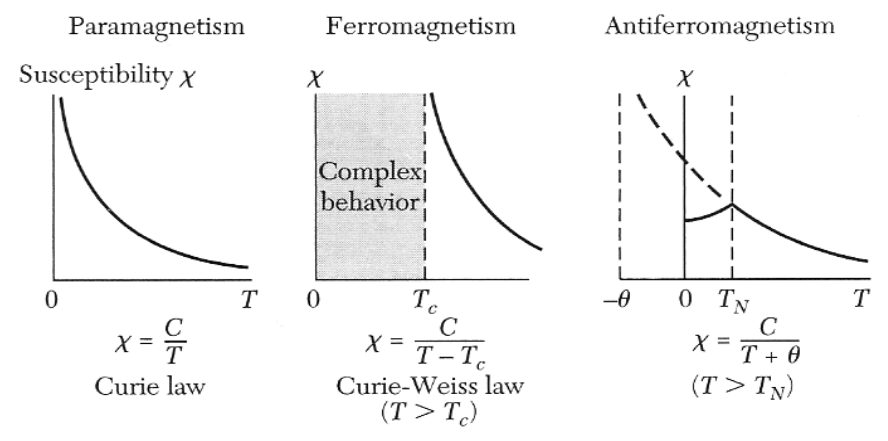


Table 2 Antiferromagnetic crystals ↑ ↓ ↑ ↓ ↑ ↓ ↑ ↓

Substance	Paramagnetic ion lattice	Transition temperature, T_N , in K	Curie-Weiss θ , in K	$\frac{\theta}{T_N}$	$\frac{\chi(0)}{\chi(T_N)}$
MnO	fcc	116	610	5.3	$\frac{2}{3}$
MnS	fcc	160	528	3.3	0.82
MnTe	hex. layer	307	690	2.25	
MnF ₂	bc tetr.	67	82	1.24	0.76
FeF ₂	bc tetr.	79	117	1.48	0.72
FeCl ₂	hex. layer	24	48	2.0	<0.2
FeO	fcc	198	570	2.9	0.8
CoCl ₂	hex. layer	25	38.1	1.53	
CoO	fcc	291	330	1.14	
NiCl ₂	hex. layer	50	68.2	1.37	
NiO	fcc	525	~2000	~4	
Cr	bcc	308			



from Kittel

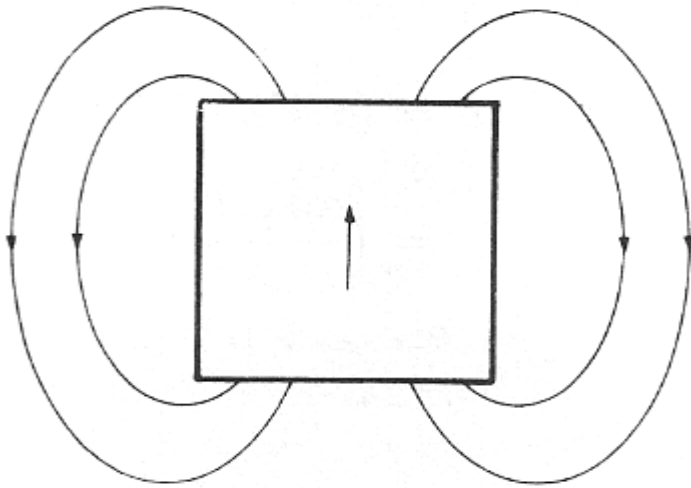
Applications of magnetism

Hard magnets: permanent magnets, motors, generators, microphones

Soft magnets: transformers

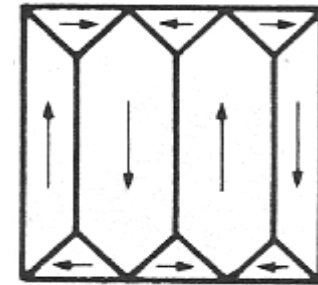
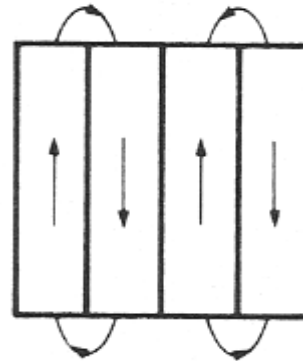
Magnetic recording

Magnetic domains (weissche Bezirke)

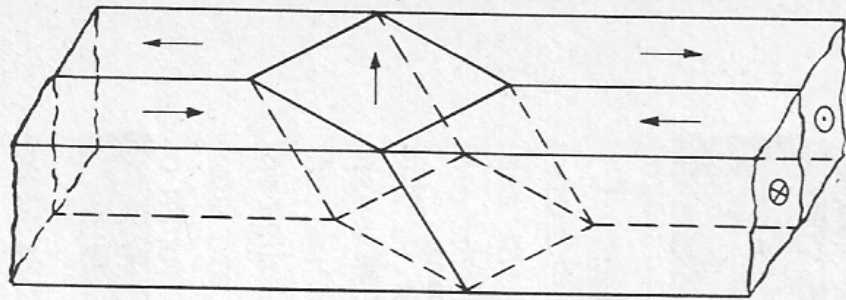


Magnetic energy density

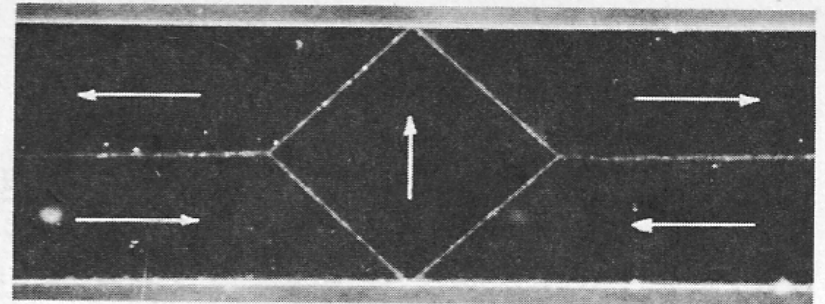
$$\frac{B^2}{2\mu_0}$$



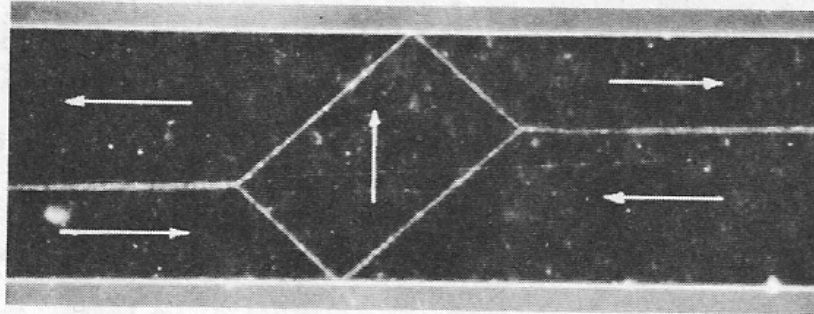
Costs energy to introduce domain walls where spin up regions are adjacent to spin down regions.



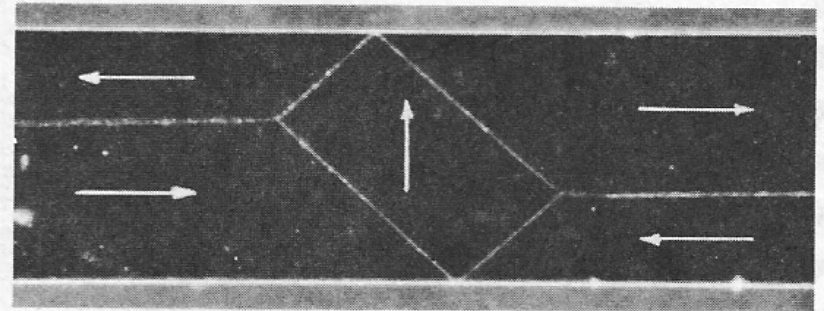
$H=0$



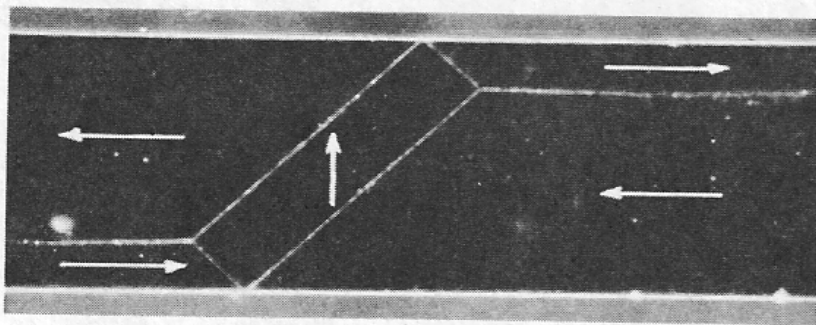
$H=0$



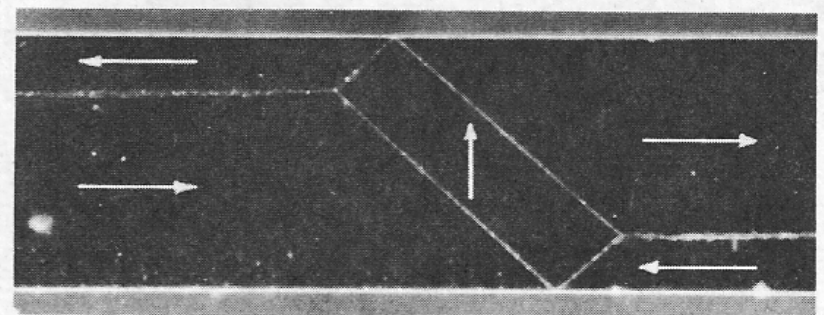
$\leftarrow H$



$H \rightarrow$



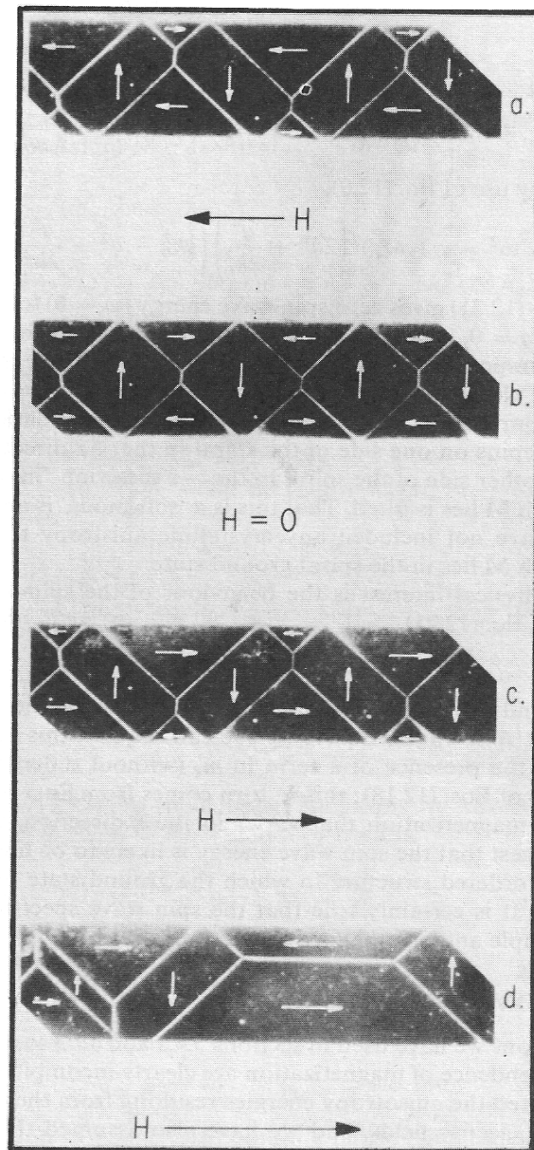
$\leftarrow H$



$H \rightarrow$

Figure 27. Photographs of diamond-shaped vortices in a channel with a magnetic field H .

Ferromagnetic domains

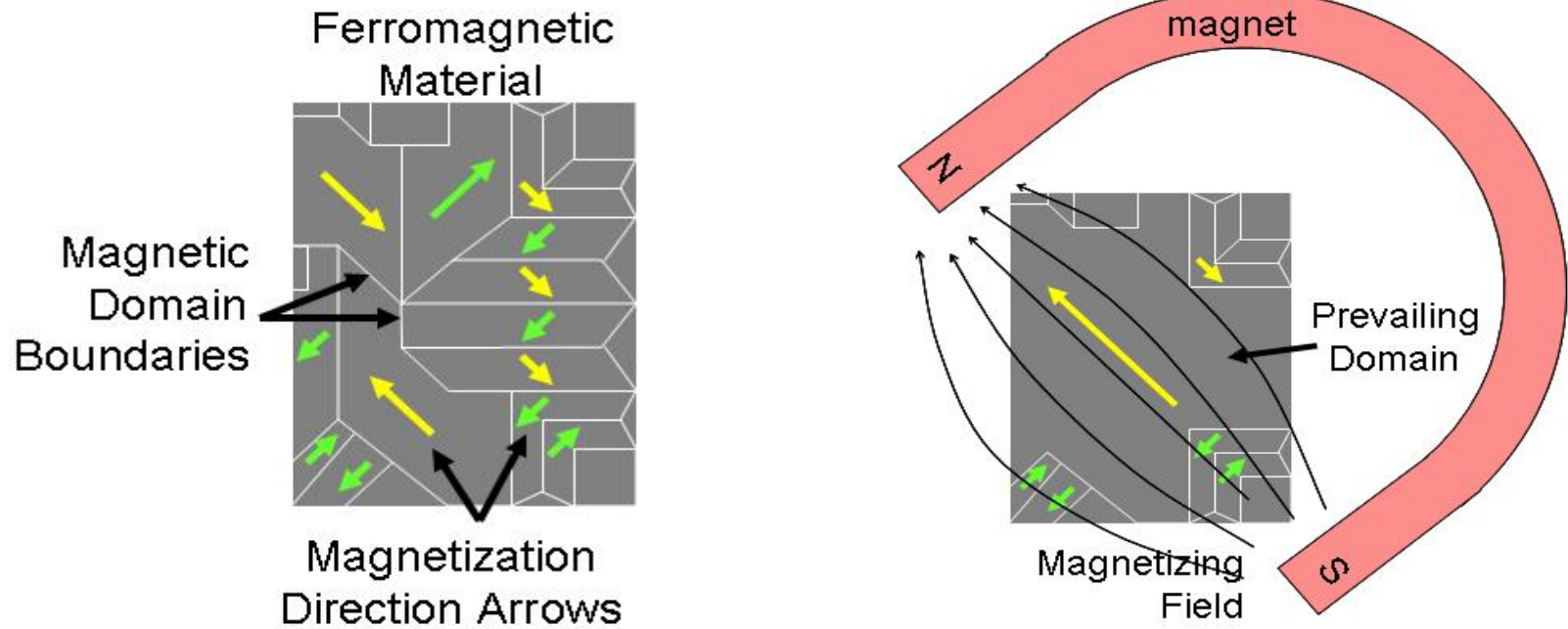


Weak fields: favorable domains expand
Strong fields: domains rotate to align with field

Irreproducible jump between c and d.

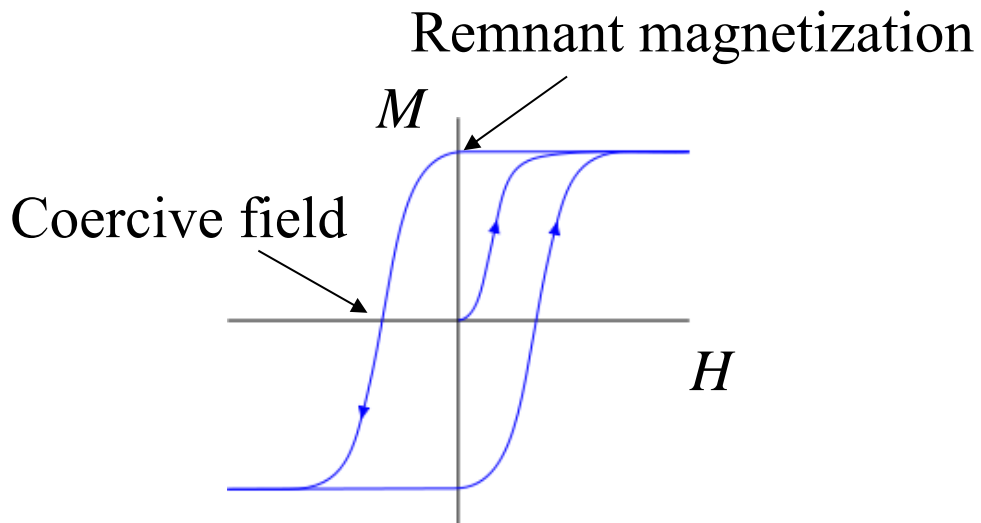
Fig. 12.5. Photographs showing reversible domain wall motion in a $50\ \mu\text{m}$ whisker from (a) to (b) to (c), with an irreversible jump from (c) to (d).
{R. W. de Blois and C. D. Graham, *J. Appl. Phys.*, **29**, 931 (1958)}.

Magnetizing a magnet



Weak fields: favorable domains expand
Strong fields: domains rotate to align with field

Hysteresis



$$B = \mu_0 (H + M)$$

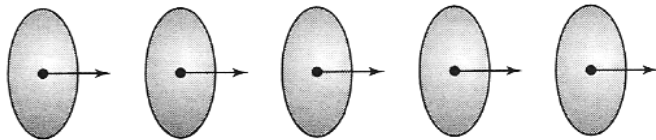
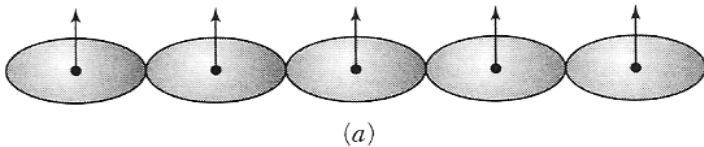
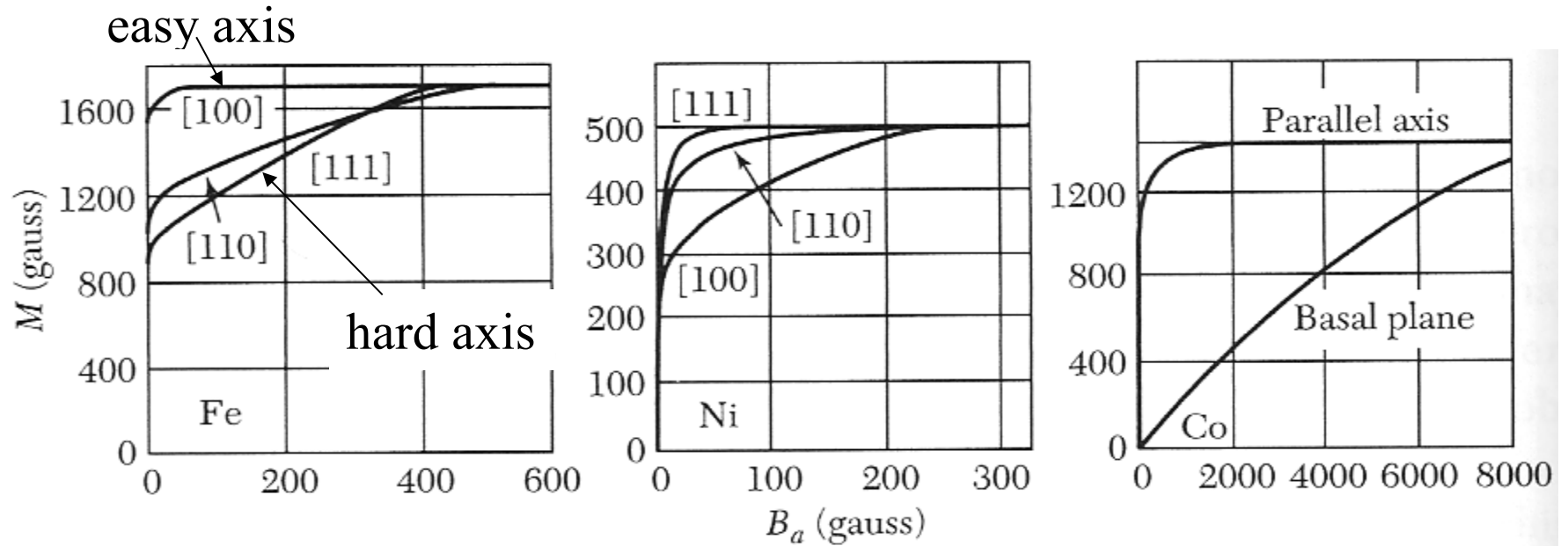
$$M = \chi H$$

$$B = \mu_0 (1 + \chi) H = \mu_r \mu_0 H$$

$$\mu_r = (1 + \chi)$$

Area of the loop is proportional to energy dissipated in traversing the loop.

Anisotropy energy



Spin-orbit coupling couples the shape of the wavefunction to the spin. The exchange energy depends on the overlap of the wavefunctions and thus on spin direction.

Bloch wall

energy of two spins

$$w = -J\vec{S}_i \cdot \vec{S}_j = -JS^2 \cos \varphi \approx -JS^2 \left(1 - \frac{\varphi^2}{2} \right)$$

neglecting the constant part

$$w \approx JS^2 \frac{\varphi^2}{2}$$

$$\varphi = \frac{\pi}{N}$$

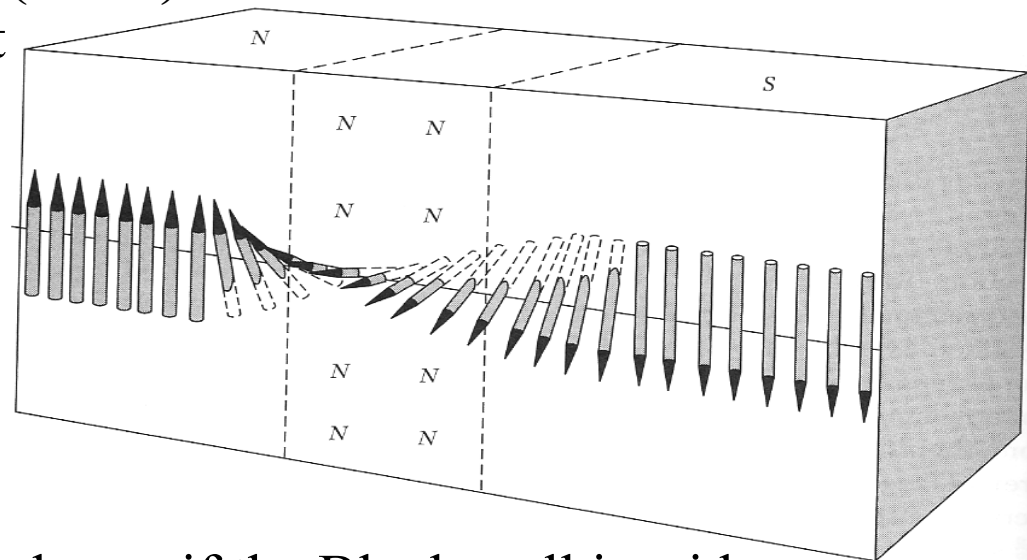
energy of a line of spins

$$Nw \approx \frac{JS^2 \pi^2}{2N}$$

energy is lower if the Bloch wall is wide

$$\text{energy per unit area} \approx \frac{JS^2 \pi^2}{2Na^2}$$

a is the lattice constant



Bloch wall

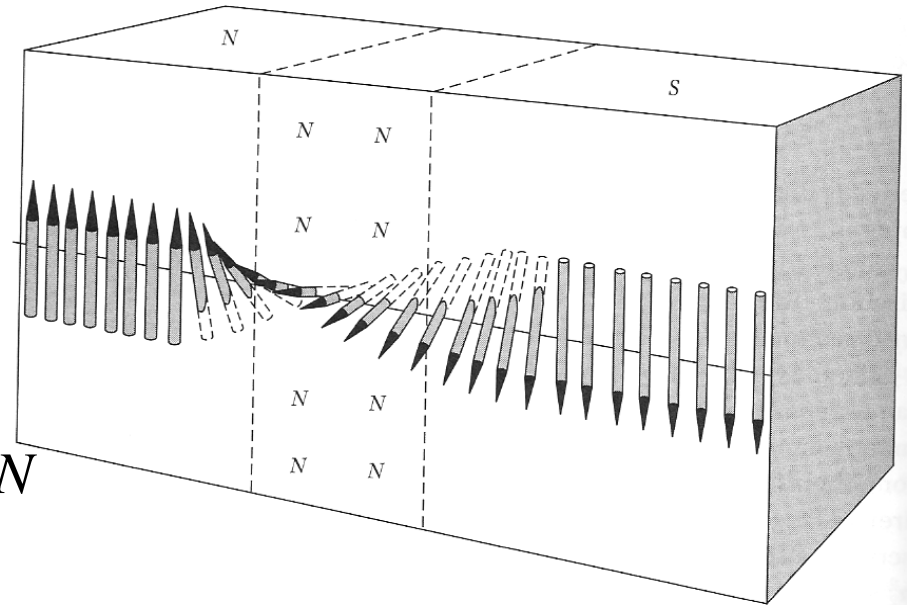
Anisotropy energy depends on the number of spins pointing in the hard direction

$\approx KNa$ ← $Na = \text{thickness of wall}$
 anisotropy constant J/m^3

Total energy per unit area:

$$E = \frac{JS^2\pi^2}{2Na^2} + KNa \quad [\text{J/m}^2]$$

smaller for large N smaller for small N



$$\frac{dE}{dN} = 0 \Rightarrow -\frac{JS^2\pi^2}{2N^2a^2} + Ka = 0$$

$$N = \sqrt{\frac{JS^2\pi^2}{2Ka^3}}$$

$N \sim 300$ for iron